

Homoleptic Complexes of Cobalt(0) and Nickel(0,I) with 1,1'-Bis(diphenylphosphino)ferrocene (dppf): Synthesis and Characterization

Giuseppe Pilloni,[†] Antonio Toffoletti,[†] Giuliano Bandoli,[‡] and Bruno Longato^{*,†,§}

Dipartimento di Scienze Chimiche, Università di Padova, Via Marzolo 1, 35131 Padova, Italy, Dipartimento di Scienze Farmaceutiche, Università di Padova, Via Marzolo 5, 35131 Padova, Italy, and Istituto di Scienze e Tecnologie Molecolari, CNR, Via Marzolo 1, 35131 Padova, Italy

Received June 28, 2006

Reduction of Co(dppf)Cl_2 with 2 equiv of sodium naphthalenide in THF, in the presence of dppf, affords the homoleptic complex Co(dppf)_2 , **1**, isolated in 65% yield as a brick red solid, extremely air sensitive. In solution, under inert atmosphere, **1** slowly decomposes into Co and dppf, following a first-order kinetic law ($t_{1/2} = 21$ h at 22 °C). Similarly to the Rh and Ir congeners, **1** undergoes a one-electron reversible reduction to $[\text{Co(dppf)}_2]^-$. Attempts to obtain this d^{10} species by chemical as well as electrochemical reduction of **1** lead to the hydride HCo(dppf)_2 , **2**, as the only product that can be isolated. Reduction of Ni(dppf)Cl_2 with sodium in the presence of dppf and catalytic amounts of naphthalene affords Ni(dppf)_2 , **3**, isolated in 60% yield as a yellow air stable solid. The stoichiometric oxidation of **3** with $[\text{FeCp}_2]\text{PF}_6$ forms the d^9 complex $[\text{Ni(dppf)}_2]\text{PF}_6$, **4**, which represents the second example of a structurally characterized Ni(I) complex stabilized by phosphines. A single-crystal X-ray analysis shows for the metal a distorted tetrahedral environment with a dihedral angle defined by the planes containing the atoms P(1), Ni, P(2) and P(3), Ni, P(4) of 78.2° and remarkably long Ni–P bond distances (2.342(3)–2.394(3) Å). The EPR spectroscopic properties of **1** (at 106 K in THF) and **4** (at 7 K in 2-methyl-THF) have been examined and *g* tensor values measured (**1**, $g_x = 2.008$, $g_y = 2.182$, $g_z = 2.326$; **4**, $g_x = 2.098$, $g_y = 2.113$, $g_z = 2.332$). A linear dependence between the hyperfine constants and the Ni–P bond distances has been evidenced. Finally, the change with time of the EPR spectrum of **4** indicates that it very slowly releases dppf.

Introduction

We have recently demonstrated that the organometallic ligand 1,1'-bis(diphenylphosphino)ferrocene (dppf) is able to stabilize iridium and rhodium atoms in their oxidation states +I, 0, and –I, and the characterization of the complexes $[\text{M(dppf)}_2]^+$, $[\text{M(dppf)}_2]^0$, and $[\text{M(dppf)}_2]^-$ (M = Ir and Rh) has been described.^{1,2} The X-ray structure analysis of these redox-related complexes provided the opportunity to study the structural changes of the $\{\text{MP}_4\}^n$ moiety on changing the charge of the complex ($n = +1, 0, -1$). The

combined analysis of the X-ray and EPR data for the d^9 species M(dppf)_2 , (M = Rh and Ir) evidenced a linear dependence of the metal–phosphorus bond distances and the coupling constants of the unpaired electron with the phosphorus nuclei. This observation suggests the possibility to correlate phosphorus coupling with the metal–phosphorus bond length in similar complexes.

In this paper we report the synthesis and characterization of related cobalt and nickel complexes. The neutral Co(0) compound, Co(dppf)_2 (**1**), and Ni(0) analogue, Ni(dppf)_2 (**3**), have been prepared by reduction of the precursors M(dppf)Cl_2 , (M = Co, Ni), while the paramagnetic Ni derivative, $[\text{Ni(dppf)}_2]\text{PF}_6$ (**4**), has been obtained by chemical oxidation of **3** with the ferrocenium salt $[\text{FeCp}_2]\text{PF}_6$. The molecular structure of **4** has been obtained by single-crystal X-ray analysis and represents a rare example among the homoleptic phosphine complexes of Ni(I) chemically characterized.³ To the best of our knowledge, only one of them, i.e., $[\text{Ni}$

* To whom correspondence should be addressed. E-mail: bruno.longato@unipd.it. Phone: +39-049-8275197. Fax: +39-049-8275161.

[†] Dipartimento di Scienze Chimiche, Università di Padova.

[‡] Dipartimento di Scienze Farmaceutiche, Università di Padova.

[§] Istituto di Scienze e Tecnologie Molecolari, CNR.

(1) Longato, B.; Riello, L.; Bandoli, G.; Pilloni, G. *Inorg. Chem.* **1999**, *38*, 2818.

(2) Longato, B.; Coppo, R.; Pilloni, G.; Corvaja, C.; Toffoletti, A.; Bandoli, G. *J. Organomet. Chem.* **2001**, *637–639*, 710.

(PMe₃)₄]⁺, has been structurally authenticated.^{3a} A detailed study of **4** by electron paramagnetic resonance spectroscopy, in 2-methyltetrahydrofuran at 7 K, confirms the linear dependence of the metal–phosphorus bond distances and the coupling constant of the unpaired electron with the phosphorus nuclei, previously evidenced for the Rh and Ir analogues.²

In addition, we show that the isolation of the anionic complex [Co(dppf)₂][−] is prevented by abstraction of a proton from the medium to give the hydride HCo(dppf)₂, **2**, which has also been isolated. Moreover, different synthetic strategies applied to the synthesis of the homoleptic cationic d⁸ species, [Co(dppf)₂]⁺ and [Ni(dppf)₂]²⁺, proved to be unsuccessful.

Experimental Section

General Procedures and Materials. All reactions and manipulations of solutions were performed under a dinitrogen atmosphere of a Braun MB150 drybox. Anhydrous tetrahydrofuran (THF), 2-methyltetrahydrofuran (Me-THF), toluene, and hexane, purchased from Aldrich, were further purified by distillation over Na/benzophenone. 1,1'-Bis(diphenylphosphino)ferrocene, dppf, was purchased from Aldrich and used as received. Electrochemical grade tetrabutylammonium perchlorate, TBAP, was obtained from Fluka and used without further purification after drying in a vacuum at 60 °C. High-purity argon, further purified from oxygen by passage over reduced copper at 450 °C, was used in the electrochemical experiments. M(dppf)Cl₂ (M = Ni, Co) were prepared as previously reported.⁴

Apparatus. ¹H and ³¹P{¹H}NMR spectra were obtained at 298 K on a Bruker Avance 300 MHz spectrometer. The external reference was H₃PO₄ (85% w/w in H₂O) for ³¹P spectra. ¹H chemical shifts are referred to the residual peak(s) of the deuterated solvents used (Aldrich). IR and electronic spectra were obtained using a Nicolet 55XC-FTIR and a Cary 5E spectrometer, respectively. EPR spectra from room temperature to 106 K were recorded with a Bruker ER 200 D X-band spectrometer equipped with a liquid-nitrogen-temperature controller, whereas low-temperature spectra (7 K) were recorded with a Bruker ECS 106 X-band spectrometer equipped with a helium flow cryostat (Oxford ESR 900). Solutions ca. 10^{−3} mol dm^{−3} of [Ni(dppf)₂]PF₆ (in Me-THF) and Co(dppf)₂ (in THF) were prepared under strict conditions of oxygen and humidity absence. The samples were placed in EPR quartz tubes connected to a vacuum line, and after several freeze–pump–thaw cycles, the tubes were sealed under vacuum.

All electrochemical experiments were performed in anhydrous deoxygenated THF solutions with 0.2 mol dm^{−3} TBAP as the supporting electrolyte, using a conventional three-electrode liquid-jacketed cell. Cyclic voltammetry (CV) measurements were performed with an Amel 551 potentiostat modulated by an Amel 566 function generator. The recording device was an Amel model 863 X-Y recorder. The working electrode was a planar platinum microelectrode (ca. 0.3 mm²) surrounded by a platinum spiral counter electrode. Controlled potential electrolyses were performed with an Amel 552 potentiostat linked to an Amel 731 digital integrator. The working electrode was platinum gauze (ca. 100 cm²), and the counter electrode was external, the connection being made

through an appropriate salt bridge. In all cases silver/0.1 mol dm^{−3} silver perchlorate in acetonitrile, separated from the test solution by 0.2 mol dm^{−3} TBAP in THF solution sandwiched between two fritted disks, was used as the reference electrode. Compensation for *iR* drop was achieved by positive feedback. Ferrocene was added at the end of each experiment as the internal reference. All potentials are referred to the ferrocenium/ferrocene redox couple (*E*_{1/2} = +0.080 V relative to the actual Ag/AgClO₄ reference electrode and +0.535 V vs aqueous SCE under the present experimental conditions).

Preparation of the Complexes. Co(dppf)₂ (1). To a suspension of Co(dppf)Cl₂ (1.121 g, 1.64 mmol) and dppf (0.908 g, 1.64 mmol) in THF (10 mL) was added 10.0 mL of a 0.33 mol dm^{−3} THF solution of sodium naphthalenide (2 equiv). The mixture was stirred at room temperature for 30 min and then filtered. Addition of hexane to the filtrate afforded a precipitate which was collected by filtration, washed with hexane, and carefully dried under vacuum to give 1.251 g of a brick red solid (yield 65%). Anal. Calcd for C₆₈H₅₆P₄Fe₂Co: C, 69.94; H, 4.83. Found: C, 70.38; H, 5.12. Visible–NIR spectrum in THF: λ_{max} 856 nm (ε = 528 M^{−1} cm^{−1}); 1395 nm (ε = 1432 M^{−1} cm^{−1}).

HCo(dppf)₂ (2). To a suspension of Co(dppf)Cl₂ (0.692 g, 1.01 mmol) and dppf (0.561 g, 1.01 mmol) in THF (12 mL) was added 13.3 mL of sodium amalgam (0.41 mol dm^{−3}, 5.46 mmol), which was then stirred at room temperature for 30 min. The solution was separated from the amalgam with a syringe and filtered. Addition of hexane to the filtrate afforded a precipitate which was collected by filtration, washed with hexane, and dried under vacuum to give 0.892 g of a red solid (yield 75%). Anal. Calcd for C₆₈H₅₇P₄Fe₂Co: C, 69.88; H, 4.92. Found: C, 70.77; H, 5.49. IR spectrum (in KBr): ν (CoH) = 1962 cm^{−1} (w). ¹H NMR (δ, ppm, in C₆D₆): 7.8–6.8 (complex multiplet, 40 H, Ph); 4.5–3.8 (c.m. 16 H, Cp); −19.5 (apparent quintet, ²J_{HP} 35 Hz, 1 H, HCo). ³¹P{¹H} NMR (in C₆D₆): δ 38.7 (broad singlet).

Ni(dppf)₂ (3). To a suspension of Ni(dppf)Cl₂ (993 mg, 1.45 mmol) and dppf (807 mg, 1.45 mmol) in toluene (40 mL) was dropwise added 20 mL of a 0.146 mol dm^{−3} THF solution of sodium naphthalenide (2.92 mmol). The reaction mixture was stirred at room temperature for 30 min and then evaporated to dryness. The residue was dissolved in C₆H₆ and filtered to eliminate small amounts of a dark solid. Addition of hexane afforded a yellow powdered solid which was recovered by filtration, washed with hexane, and dried under vacuum to give 1.1 g of Ni(dppf)₂ (yield 60%). Anal. Calcd for C₆₈H₅₆P₄Fe₂Ni: C, 69.96; H, 4.83. Found: C, 69.06; H, 4.79. ¹H NMR (δ, ppm, in C₆D₆): 7.77 (broad singlet, 16 H, Ph); 6.90 (br s, 24 H, Ph); 4.24 (br s, 8 H, Cp); 3.96 (br s, 8 H, Cp). ³¹P NMR (in C₆D₆): δ 14.98 s. Yellow-orange crystals of **3**, obtained from a benzene solution by layering hexane, were not appropriate for a X-ray determination.

[Ni(dppf)₂]PF₆ (4). A mixture of Ni(dppf)₂ (1.034 g, 0.88 mmol) and [Fe(C₅H₅)₂]PF₆ (282 mg, 0.85 mmol) was dissolved in THF (20 mL) and stirred at room temperature for 12 h. The resulting yellow-green precipitate was recovered by filtration, washed with hexane, and dried under vacuum to give 1.01 g of **4** (yield 90%). Purification of the crude product by dissolution in acetone/THF (2:1) and precipitation by addition of hexane afforded green microcrystals. Anal. Calcd for C₆₈H₅₆P₅F₆Fe₂Ni: C, 62.20; H, 4.30. Found: C, 61.48; H, 4.82. ³¹P NMR (in acetone-*d*₆): δ −144.3 (septuplet, ¹J_{PF} = 710 Hz, PF₆[−]). Visible–NIR spectrum in THF: λ_{max} ca. 1600 nm (ε = 118 M^{−1} cm^{−1}).

X-ray Data Collection and Processing. Suitable black crystals of the d⁹ species, analyzing as [Ni(dppf)₂]PF₆·2C₆H₅CH₃, were obtained by layering hexane into a toluene/THF (9:1 v/v) solution

(3) (a) Gleizes, A.; Dartiguenave, M.; Dartiguenave, Y.; Galy, J. *J. Am. Chem. Soc.* **1977**, *99*, 5187. (b) Holah, D. G.; Hughes, A. N.; Hui, B. C.; C.-T. Kan, C.-T. *Can. J. Chem.* **1978**, *56*, 2552.

(4) Corain, B.; Longato, B.; Favero, G.; Ajò, D.; Pilloni, G.; Russo, U.; Kreissl, F. R. *Inorg. Chim. Acta* **1989**, *157*, 259.

Table 1. Crystallographic Data for [Ni(dppf)₂](PF₆)·2C₇H₈

chem formula	C ₈₂ H ₇₂ F ₆ Fe ₂ NiP ₅
fw	1496.7
cryst system	orthorhombic
space group	<i>Pbca</i> (No. 61)
unit cell dims	
<i>a</i> (Å)	24.210(4)
<i>b</i> (Å)	21.279(5)
<i>c</i> (Å)	27.345(6)
<i>V</i> (Å ³)	14087(5)
<i>Z</i>	8
ρ _{calc} (g cm ⁻³)	1.411
μ(Mo Kα) (mm ⁻¹)	8.46
scan type	ω-2θ
2θ _{max} (deg)	45
measd reflns	9199
obsd reflns [<i>I</i> > 2σ(<i>I</i>)]	5803
refined params	767
R(<i>F</i> _o) ^a	0.079
wR(<i>F</i> _o ²) ^b	0.139
goodness-of-fit	1.135

$$^a R = \sum ||F_o| - |F_c|| / \sum |F_o|. \quad ^b wR = [\sum w(|F_o|^2 - |F_c|^2)^2] / \sum w|F_o|^2]^{1/2}.$$

Table 2. Selected Bond Lengths and Contact Distances (Å) and Angles (deg) for [Ni(dppf)₂](PF₆)·2C₇H₈

Ni–P(1)	2.368(3)	Fe(1)–X(1) ^a	1.636(4)
Ni–P(2)	2.342(3)	Fe(1)–X(2) ^a	1.646(4)
Ni–P(3)	2.394(3)	Fe(2)–X(3) ^a	1.629(4)
Ni–P(4)	2.376(3)	Fe(2)–X(4) ^a	1.645(5)
P(1)–C(1)	1.84(1)	P(1)→P(2)	3.586(7)
P(2)–C(6)	1.80(1)	P(3)→P(4)	3.668(7)
P(3)–C(11)	1.82(1)	P(1)→P(4)	3.877(8)
P(4)–C(16)	1.84(1)	P(2)→P(3)	3.750(7)
P(1)–Ni–P(2)	99.2(1)	Fe(1)–C(1)–P(1)	130.2(6)
P(3)–Ni–P(4)	100.5(1)	Fe(1)–C(6)–P(2)	125.0(6)
Ni–P(1)–C(1)	118.3(4)	Fe(2)–C(11)–P(3)	126.1(6)
Ni–P(2)–C(6)	116.6(4)	Fe(2)–C(16)–P(4)	130.7(6)
Ni–P(3)–C(11)	115.2(4)	C(1)–Fe(1)–C(6)	109.9(5)
Ni–P(4)–C(16)	117.1(4)	C(11)–Fe(2)–C(16)	111.2(4)

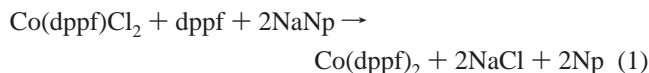
^a Distances of Fe atom from the centroid (X) of Cp rings.

of **4**. Data collection used a STOE four-circle diffractometer, and many of the details of the structure analysis are listed in Table 1. The selected crystal was coated with mineral oil and sealed in a glass capillary tube. The crystal was slightly sensitive toward X-rays and decomposed after prolonged irradiation. The decay in intensity was up to 10% during data collection. Scans round the diffraction vector of several strong reflections showed some variation in intensity, but owing to the decay, absorption correction was not applied.

The structure was solved by heavy-atom Patterson methods and expanded using Fourier techniques to locate all non-H atoms. During refinement, performed on *F*², it became apparent that the PF₆ anion was suffering from high thermal parameters and a Fourier-difference map revealed several small maxima in the vicinity of the toluene molecules, indicating positional disorder. However, efforts to identify alternative sites for these atoms were not successful and hence the toluene molecules were treated as rigid groups. As a result of this severe disorder, the diffraction data were of rather poor quality; the diffracting ability of the sample fell off rapidly with increasing Bragg angle (observed reflections only 63% of the total), and presumably the unresolved disorder is responsible for the high R values. In any case, the final difference map was featureless, the largest peak being of 0.64 e Å⁻³, around the toluene molecules. Selected bond lengths and angles are listed in Table 2. The structure was solved and refined using the SHELXTL NT suite of programs.⁵

Results and Discussion

Synthesis and Characterization of the Co(0) Complex, Co(dppf)₂ (1). Addition of the stoichiometric amount of sodium naphthalenide (NaNp) to a THF suspension of Co(dppf)Cl₂, in the presence of dppf, forms immediately a deep-red solution of **1**, according to eq 1:



Separation of the sodium chloride followed by the rapid precipitation with hexane allowed the isolation of **1** as a brick-red solid, very air sensitive, which has been characterized by elemental analysis, vis-NIR, and EPR spectra. In THF, a fresh solution of **1** displayed two absorption bands at λ_{max} 856 and 1395 nm, whose intensities slowly decreased with time due to decomposition into dppf and metallic cobalt. With monitoring of the intensities of these bands, both in the absence and in the presence of added dppf, a first-order kinetic law has been observed (*t*_{1/2} = 21 h, at 22 °C).

As expected for a homoleptic zerovalent cobalt phosphine complex,⁶ **1** undergoes an essentially reversible one-electron reduction to Co(–I) species and two discrete oxidation processes to Co(I) and Co(II) derivatives. Representative cyclic voltammograms are shown in Figure 1a,b.

An inspection of the voltammetric profile reveals that the reduction product [Co(dppf)₂][–], unlike the Rh and Ir analogues,^{1,2} is unstable in the CV time scale. In fact, electrochemical reduction of **1**, as well as chemical reduction of Co(dppf)Cl₂ with an excess of Na amalgam in the presence of dppf, gave a deep red solution of the hydride HCo(dppf)₂, **2**. Complex **2** has been characterized by elemental analysis and IR and NMR spectra. In the IR spectrum the Co–H stretching is observed as a single weak absorption at 1962 cm⁻¹. In the ¹H NMR spectrum the hydride resonance occurs as a quintet (²*J*_{HP} 35 Hz) at δ –19.5 ppm indicative of a pentacoordinate metal center having two chelated, magnetically equivalent, dppf ligands. Accordingly, in the proton-decoupled ³¹P NMR spectrum the phosphines exhibit a single resonance at δ 37.8.

As far as the oxidation pattern of **1** is concerned, attempts to ascertain the viability of the homoleptic complexes [Co(dppf)₂]⁺ and [Co(dppf)₂]²⁺, closely related to the well-known 1,2-bis(diphenylphosphino)ethane (dppe) derivatives,⁷ by controlled potential electrolyses proved to be unsuccessful in that the resulting spent anolytes exhibited electrochemical features quite different from those observed in precursor **1**. A similar failure resulted in the chemical oxidation of complex **1**.

Synthesis of the Ni(0), Ni(dppf)₂ (3), and Ni(I), [Ni(dppf)₂]⁺PF₆ (4), Complexes. Following the procedure described for the Co analogue, the Ni(0) complex Ni(dppf)₂,

- (5) Sheldrick, G. M. *SHELXTL NT*, ver. 5.10; Bruker AXS Inc.: Madison, WI, 1997.
- (6) Pilloni, G.; Zotti, G.; Martelli, M. *J. Electroanal. Chem.* **1974**, *50*, 295.
- (7) Nobile, C. F.; Rossi, M.; Sacco, A. *Inorg. Chim. Acta* **1971**, *5*, 698 and ref. therein.

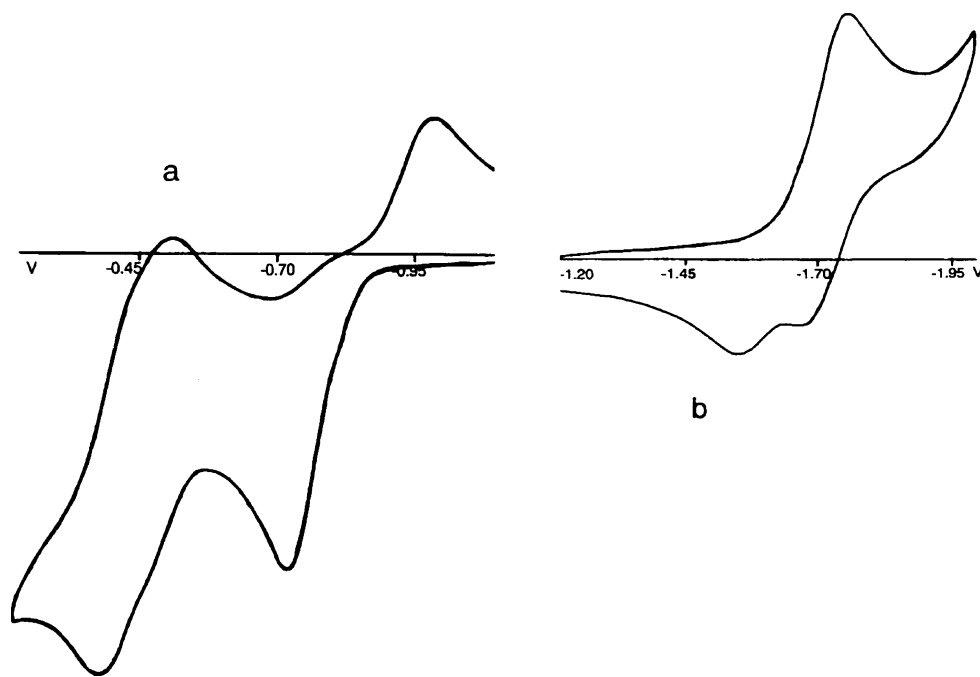


Figure 1. Cyclic voltammograms of a fresh solution 3.0 mM of Co(dppf)_2 , **1**, in THF, TBAP 0.2 M, at 25 °C, with scan rate 100 mV/s, vs ferrocenium/ferrocene reference: (a) oxidation mode; (b) reduction mode.

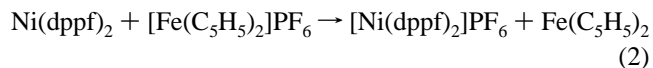
3, has been isolated in fairly good yield. The reduction of the Ni(II) complex is accompanied by the formation of small amounts of black solid, likely Ni in colloidal form. This side reaction can be partially avoided by reducing Ni(dppf)Cl_2 with Na in the presence of catalytic amounts of naphthalene. The crystals obtained by vapor diffusion of hexane into a saturated solution of **3** were not appropriate for a X-ray diffraction study. The compound appears to be air stable in the solid phase while in benzene or toluene it is indefinitely stable only under inert atmosphere. Moreover, the complex is unstable in chlorinated solvents. For instance, addition of CHCl_3 (a few percent) to a benzene solution of **3** determines the immediate formation of a precipitate which was not further investigated. The solid is likely the product of an oxidative addition of CHCl_3 to complex **3**, in line with previous observations on other Ni(0) phosphine complexes.⁸

The ^1H NMR spectrum of **3** shows, in addition to the resonances due to the phenyl groups, two unresolved multiplets, attributable to the cyclopentadienyl protons, at $\delta = 4.24$ and 3.96 ppm. The corresponding ^{31}P NMR spectrum is characterized by a sharp singlet at $\delta 15.02$, in agreement with the presence of chemically and magnetically equivalent dppf molecules bonded to a d^{10} metal center. The coordination chemical shift of the dppf ligand ($\Delta\delta = \delta_{\text{complex}} - \delta_{\text{dppf}} = 33.01$ ppm) is in line with the values found in other Ni(0) diphosphine complexes.⁹

CV tests in THF show that the d^{10} species undergoes a fully reversible one-electron oxidation step centered at $E_{1/2} = -1.175$ V, as mean value of the potentials for positive and negative peak currents, to give the species $[\text{Ni(dppf)}_2]^+$, **4**. A typical voltammogram is shown in Figure 2.

Exhaustive electrolysis at potentials past the anodic peak results in the removal of one electron/molecule of depolarizer to give a greenish solution with a voltammetric reduction profile virtually complementary to the oxidation pattern of the precursor, thus raising in evidence the chemical reversibility of the electron-transfer process. In the anodic scan of the voltage, as expected for a Ni(I) derivative, an oxidation peak is displayed. However, this signal occurs at far more anodic potential values ($E_p = -0.25$ V) when compared with that of the d^{10} parent and its profile is that anticipated for a totally irreversible charge-transfer reaction. This pattern appears to be in striking contrast with that exhibited by the strictly related dppe complex¹⁰ and it questions the viability of the cationic d^8 species $[\text{Ni(dppf)}_2]^{2+}$ (see below).

As anticipated on the basis of the electrochemical analysis, complex **4** can be conveniently prepared by oxidation of **3** with the ferrocenium ion, according to eq 2:



In THF the reaction occurs in ca. 12 h and the moderate solubility of **4** allows its isolation by a simple filtration of the green solid separated. The NIR spectrum of **4** in THF exhibits a maximum at $\lambda = 1600$ nm with $\epsilon = 118 \text{ M}^{-1} \text{ cm}^{-1}$, in good agreement with the value reported for $[\text{Ni}(\text{PPh}_3)_4]^+$.^{3b}

Control experiments confirm the electrochemical suggestions on the instability of the homoleptic cationic d^8 species, $[\text{Ni(dppf)}_2]^{2+}$. As a matter of fact, addition of 1 equiv of the ferrocenium salt to a THF solution of **4** gives rise to the decomposition of the oxidation product as inferred by the

(8) Tsou, T. T.; Kochi, J. K. *J. Am. Chem. Soc.* **1979**, *101*, 6319 and reference therein.

(9) Garrou, P. E. *Chem. Rev.* **1981**, *81*, 229.

(10) Martelli, M.; Pilloni, G.; Zotti, G.; Daolio, S. *Inorg. Chim. Acta* **1974**, *11*, 155.

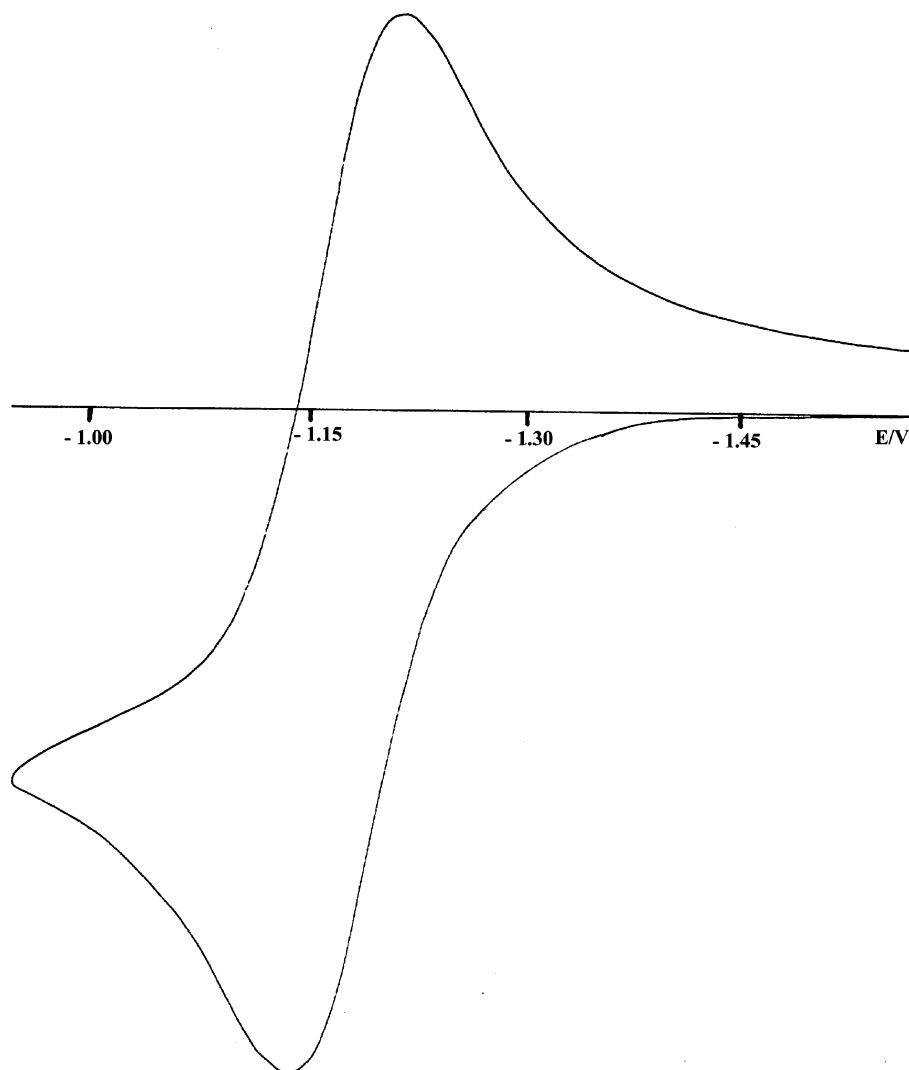


Figure 2. Cyclic voltammogram for oxidation of a solution 9.0 mM of Ni(dppf)₂, in THF, TBAP 0.2 M, at 25 °C, with scan rate 200 mV/s, vs ferrocenium/ferrocene reference.

presence in the ³¹P NMR spectrum of the crude reaction product of the only resonance at -17.9 ppm, distinctive of uncoordinated dppf ligand.

X-ray Structure of [Ni(dppf)₂]PF₆. The ORTEP¹¹ representation and the numbering scheme of the complex are illustrated in Figure 3, and the relevant bond distances and angles are reported in Table 2.

The Ni atom is four-coordinate and the geometry around the metal is essentially tetrahedral, the dihedral angle between the P(1)–Ni–P(2) and P(3)–Ni–P(4) planes being 78.2°. The Ni–P bond lengths range between 2.342(3) and 2.394(3) Å, with an average of 2.370(3) Å. A search in the Cambridge Crystallographic Database (version 5.27 of Nov 2005 + 1 update)¹² for Ni(I) complexes (coordination number = 4) shows that the mean Ni–P bond length calculated over 14 structures is 2.253 Å. The same search shows that the longest Ni–P distance found in **4** is also the fifth longest Ni–P distance recorded so far for tetracoordinated nickel.

A more appropriate comparison should be limited to the Ni complexes containing the dppf ligand: about 10 Ni(II) structures have been reported so far. In Ni(dppf)Cl₂¹³ and Ni(dppf)Br₂¹⁴ the Ni environment is tetrahedral and the mean Ni–P distance is 2.290(9) Å. In the remaining structures, the metal is bound to another bidentate ligand and the geometry around the metal becomes square planar, with a mean Ni–P bond length of 2.211(3) Å.^{15–20} This contraction of the Ni–P bond length is consistent with the one observed

(11) Johnson, C. K. *ORTEP*; Report ORNL-5138; Oak Ridge National Laboratory: Oak Ridge, TN, 1976.
 (12) Allen, F. H. *Acta Crystallogr. B* **58** **2002**, 380–388 [Cambridge Structural Database (version 5.27 of Nov 2005 + 2 updates)].

(13) Butler, J. R.; Cullen, W. R.; Kim, T.-J.; Rettig, S. J.; Trotter, J. *Organometallics* **1985**, *4*, 972.
 (14) Casellato, U.; Ajò, D.; Valle, G.; Corain, B.; Longato, B.; Graziani, R. *J. Crystallogr. Spectrosc. Res.* **1988**, *18*, 583.
 (15) Pastorek, R.; Trávníček, Z.; Maarek, J.; Dastych, D.; Z. Sindelá, Z. *Polyhedron* **2000**, *19*, 1713.
 (16) Kamenicek, J.; Pastorek, R.; Sykora, J.; Kratochvil, B. *Acta Univ. Palacki. Olomuc.* **2000**, *39*, 45.
 (17) Pastorek, R.; Kamenicek, J.; Sindelá, Z.; Zak, Z. *Pol. J. Chem.* **2001**, *65*, 363.
 (18) Pastorek, R.; Kamenicek, J.; Pavlicek, M.; Husarek, J.; Sindelá, Z.; Zak, Z. *J. Coord. Chem.* **2002**, *55*, 1301.
 (19) Pawlas, J.; Nakao, Y.; Kawasutra, M.; Hartwig, J. F. *J. Am. Chem. Soc.* **2002**, *124*, 3669.
 (20) Arulsamy, N.; Bohle, D. S.; Imonigie, J. A.; Levine, S. *Angew. Chem., Int. Ed.* **2002**, *41*, 2371.

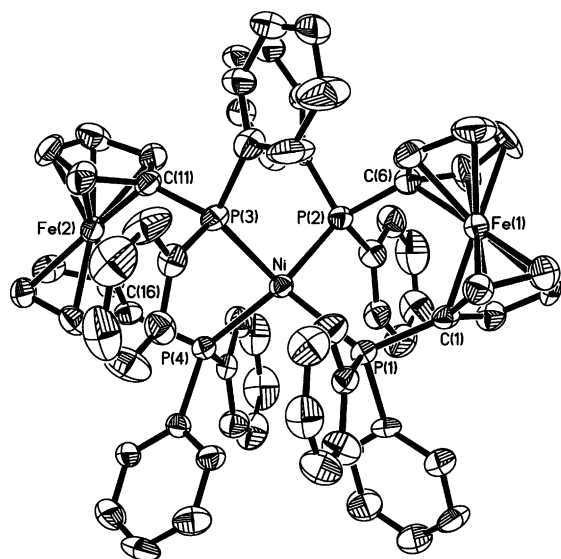


Figure 3. Crystal structure of $[\text{Ni}(\text{dppf})_2]\text{PF}_6 \cdot 2\text{C}_7\text{H}_8$, **4**. Thermal ellipsoids are drawn at the 40% probability level. The asymmetric unit of the structure comprises one $[\text{Ni}(\text{dppf})_2]^+$ cation balanced by the PF_6^- anion, along with two molecules of the recrystallization solvent. The hydrogen atoms, the anion, and the crystallization solvent molecules have been omitted in this view.

comparing tetrahedral dichlorobis(triphenylphosphine)nickel(II) ($\text{Ni}-\text{P} = 2.320(9) \text{ \AA}$) and square-planar *trans*-dichlorobis(triphenylphosphine)nickel(II)· $2\text{C}_2\text{H}_4\text{Cl}_2$ ($\text{Ni}-\text{P} = 2.242(3) \text{ \AA}$).²¹

As anticipated, the coordination environment of Ni(I) in **4** is almost tetrahedral and the unusually long bond distance of 2.370 \AA (average) observed is attributable to the steric crowding of the two bulky dppf ligands, which is also likely responsible for the moderate stability of the complex in solution (see below). In **4** the dppf molecules assume the *synclinal staggered* arrangement, the most frequent conformation for this chelated ligand. The parameters describing the ferrocenyl moieties (τ , θ , $X_A-\text{Fe}-X_B$, $\text{P}-\text{Fe}-\text{P}$), are collected in Table 3, along with those of $[\text{M}(\text{dppf})_2]^n$ ($\text{M} = \text{Rh}, \text{Ir}; n = +1, 0, -1$) previously reported.^{22–24} With respect to the parameters involving the metal center, there is a good agreement with the data found for the neutral $\text{Rh}(\text{dppf})_2^2$ and $\text{Ir}(\text{dppf})_2^1$ derivatives, especially those regarding the $\text{P}-\text{M}-\text{P}$ and γ parameters, the latter angle measuring how much the coordination around M deviates from an ideal tetrahedron ($\gamma = 90^\circ$). The value found in **4** ($\gamma = 78.2^\circ$) is similar to those found for $\text{Rh}(\text{dppf})_2$ (75.2°) and $\text{Ir}(\text{dppf})_2$ (74.7°), in line with the fact that in these complexes Ni, Rh, and Ir have the same number of valence electrons.

EPR Study of $\text{Co}(\text{dppf})_2$ and $[\text{Ni}(\text{dppf})_2]\text{PF}_6$. A freshly prepared solution of $\text{Co}(\text{dppf})_2$ (ca. $2 \times 10^{-3} \text{ M}$ in THF) does not give an EPR spectrum at room temperature. However, in frozen matrix at 106 K, the same sample gives the spectrum shown in Figure 4 along with the simulation (dashed line).

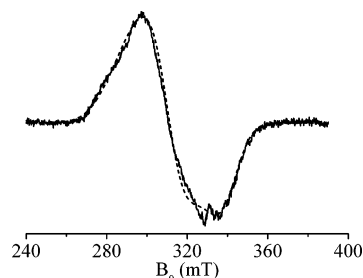


Figure 4. Experimental (solid line) and calculated (dashed line) EPR spectra of $\text{Co}(\text{dppf})_2$ ca. $2 \times 10^{-3} \text{ M}$ in THF at 106 K.

The broad signal consistent with a d^9 metal center ($S = 1/2$) has a scarcely resolved hyperfine structure so that it has been reproduced taking into account only the anisotropy of the Zeeman interaction. The simulation has been obtained with the \mathbf{g} tensor values, $g_x = 2.008$, $g_y = 2.182$, and $g_z = 2.326$, similar to the elements recently reported for the complex $\text{Co}(\text{tropp}^{\text{ph}})_2$ ($\text{tropp}^{\text{ph}} = \text{tropyliene phosphane}$).²⁵

As far as the Ni(I) derivative is concerned, at room temperature a freshly prepared solution of $[\text{Ni}(\text{dppf})_2]\text{PF}_6$ (ca. 10^{-3} M in Me-THF) does not show any EPR signal, similarly to $\text{Co}(0)$ complex **1**. This is not surprising since the absence of EPR signal in liquid solution has been already reported for other phosphine complexes of Ni(I).^{10,26} The failure to observe the EPR spectrum is attributed to the fast electron spin relaxation of the Ni(I) unpaired electron. The same sample was examined at low temperature (7 K) and gave the EPR spectrum shown in Figure 5 (solid line) along with a spectrum (dashed line A) simulated using the parameters reported in Table 4. The spectrum is almost axial ($g_x \approx g_y$) and indicates the presence of four not equivalent ^{31}P nuclei coupled with the unpaired electron of the Ni(I) species, as supported by the five-component hyperfine structure present both in the g_z and the g_x, g_y features. The spectrum calculation included the anisotropy of the \mathbf{g} tensor and only the isotropic contribution to the hyperfine coupling with the four ^{31}P nuclear spins, following a procedure previously applied for strictly related complexes.²

The calculated spectrum reproduces quite satisfactory the experimental one, despite the approximation used, with \mathbf{g} tensor values falling in the range 2.098–2.332. The average value for **4** (2.181), although similar to that found in **1** (2.172), is significantly larger than those of other diphosphine Ni(I) complexes (for instance in $[\text{Ni}(\text{dpe})_2]^+$ $g = 2.07$).^{26,27} Concerning the hyperfine constants a , the comparison with the same type of complexes ($a = \text{ca. } 168 \text{ MHz}$) reveals that our values are quite smaller (average $a = \text{ca. } 104 \text{ MHz}$). We believe that such discrepancy is related to the unusually long Ni(I)–P bonds found in **4**.

However, some differences between experimental and calculated spectra are visible: in the simulation A (Figure 5) the g_z feature exhibits a too low intensity and in the region

(21) Corain, B.; Longato, B.; Angeletti, R.; Valle, G. *Inorg. Chim. Acta* **1985**, *104*, 15.

(22) Di Noto, V.; Valle, G.; Zarli, B.; Longato, B.; Pilloni, G.; Corain, B. *Inorg. Chim. Acta* **1995**, *233*, 165.

(23) Casellato, U.; Corain, B.; Graziani, R.; Longato, B.; Pilloni, G. *Inorg. Chem.* **1990**, *29*, 1193.

(24) Bandoli, G.; Dolmella, A. *Coord. Chem. Rev.* **2000**, *209*, 161.

(25) Deblon, S.; Liesum, L.; Harmer, J.; Schönberg, H.; Schweiger, A.; Grützmacher, H. *Chem. Eur. J.* **2002**, *8*, 601.

(26) Miedaner, A.; Haltiwanger, R. C.; Du Bois, D. L. *Inorg. Chem.* **1991**, *30*, 417.

(27) Bowmaker, G. A.; Boyd, P. D. W.; Campbell, G. K.; Hope, J. M.; Martin, R. L. *Inorg. Chem.* **1982**, *21*, 1152.

Table 3. Relevant Structural Parameters for Mononuclear Neutral and Charged $[M(dppf)_2]$ Complexes Containing Two η^2 -Chelating dppf Ligands^a

complex	τ (deg)	Θ (deg)	$X_A \cdots Fe \cdots X_B$ (deg)	$P \cdots Fe \cdots P$ (deg)	M–P (Å)	P–M–P (deg)	$Fe \cdots M$ (Å)	γ (deg)	ref
$[Rh(dppf)_2]^+$	35.4, 24.1	7.5, 2.9	176.1, 178.3	60.9, 59.1	2.312(1), 2.407(4), 2.358(3), 2.321(3)	94.0(1), 92.8(2)	4.45, 4.44	49.7	22
$Rh(dppf)_2$	39.1, 18.5	2.9, 1.7	179.5, 179.1	64.2, 60.6	2.306(1), 2.323(1), 2.312(1), 2.318(1)	102.2(1), 97.6(1)	4.32, 4.32	75.2	2
$[Rh(dppf)_2]^-$	38.7, 21.2	2.7, 2.5	177.8, 179.1	62.9, 60.0	2.230(5), 2.250(5), 2.244(5), 2.251(5)	105.1(2), 100.2(2)	4.27, 4.23	95.0	2
$[Ir(dppf)_2]^+$	34.8, 25.1	9.4, 4.9	176.1, 179.9	61.1, 59.3	2.317(6), 2.389(5), 2.337(5), 2.343(6)	95.0(2), 93.6(2)	4.44, 4.43	51.0	23
$Ir(dppf)_2$	38.4, 18.7	4.4, 2.5	179.0, 178.9	63.3, 59.6	2.296(3), 2.326(3), 2.301(4), 2.315(3)	102.1(1), 97.6(1)	4.37, 4.37	74.7	1
$[Ir(dppf)_2]^-$	38.0, 22.9	3.6, 3.4	177.8, 177.7	62.1, 59.6	2.242(3), 2.256(3), 2.254(3), 2.270(3)	104.8(1), 99.8(1)	4.33, 4.28	95.0	1
$[Ni(dppf)_2]^+$	25.5, 21.1	1.5, 1.9	178.5, 177.5	62.4, 63.8	2.368(3), 2.342(3), 2.394(3), 2.376(3)	99.2(1), 100.5(1)	4.31, 4.30	78.2	present work

^a τ is the $C_A \cdots X_A \cdots X_B \cdots C_B$ torsion angle. C_A is the carbon atom of Cp ring "A" bonded to the P atom; X_A is the Cp ring "A" centroid. C_B and X_B indicate the same positions in Cp ring "B". Θ is the dihedral angle between the mean planes through the Cp rings. γ is the dihedral angle defined by the P(1)–M–P(2) and the P(3)–M–P(4) planes, where P(1) and P(2) are the donor atoms of a dppf ligand and P(3) and P(4) are those of the other.

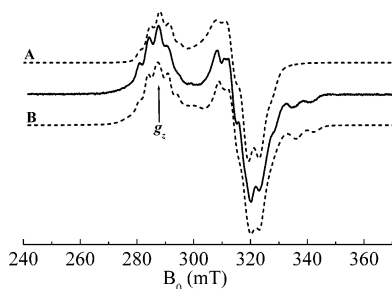


Figure 5. Experimental (solid line) EPR spectrum of a fresh sample of $[Ni(dppf)_2]PF_6$ ca. 10^{-3} M in Me-THF at 7 K. Simulated spectra (calculated with parameters of Table 4) were obtained neglecting (dashed line A) and considering (dashed line B) the presence of the species $[Ni(dppf)(Me-THF)_x]^+$.

Table 4. Hyperfine Coupling Constants (MHz) and g Values^a for $[Ni(dppf)_2]PF_6$ at 7 K

param	fresh soln				about 1 month later	
	P(1) ^b	P(2)	P(3)	P(4)	P_a	P_b
a	106	128	87	96	165	188
g_x	2.098				2.012	
g_y	2.113				2.235	
g_z	2.332				2.395	

^a Estimated errors of the coupling constants a are ± 1 MHz and of g elements are ± 0.001 . ^b The P nuclei labels are the same used in Figure 3 and Table 2. Regarding the assignment of the hyperfine constants to the four P nuclei, see the last paragraph of the EPR discussion section.

between 330 and 350 mT two weak peaks are lacking. These disagreements have been observed in different samples and become more evident after several days at room temperature, suggesting the presence of a second paramagnetic species, tentatively formulated as $[Ni(dppf)(Me-THF)_x]^+$, resulting from a slow and irreversible decomposition of the $[Ni(dppf)_2]^+$ cation. Accordingly, the spectrum of the sample left in the sealed EPR tube at room temperature for several weeks, and recorded again at 7 K, is shown in Figure 6a (solid line). The simulation (Figure 6a, dashed line) has been calculated by taking into account the hyperfine interaction with only two nonequivalent ^{31}P nuclei with the hyperfine constants reported in Table 4. This result strongly suggests that the initial complex $[Ni(dppf)_2]^+$ decomposes quantitatively but with a rate slow enough to allow its crystallization as a pure compound. It is worth to note that the solution containing the decomposition product gives an EPR signal also at 295 K, which is depicted in Figure 6b (solid line). It displays a well-resolved hyperfine structure caused by coupling to two ^{31}P nuclei with $a_P = 182$ MHz and with $g = 2.179$.

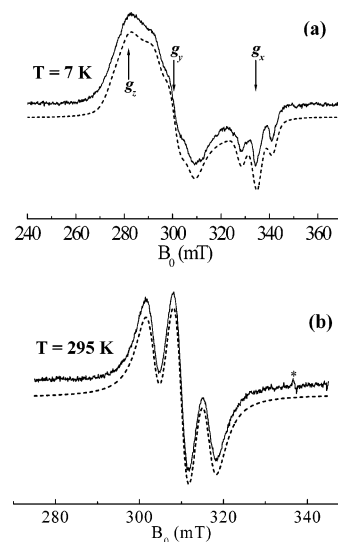


Figure 6. EPR spectra of a $[Ni(dppf)_2]PF_6$ solution (ca. 10^{-3} M in Me-THF) about 1 month after the preparation of the sample: (a) at 7 K; (b) at 295 K. The simulated spectra, calculated with the parameters reported in Table 4, are shown with dashed lines. The weak signal (asterisk) is due to the standard used for g factor calibration.

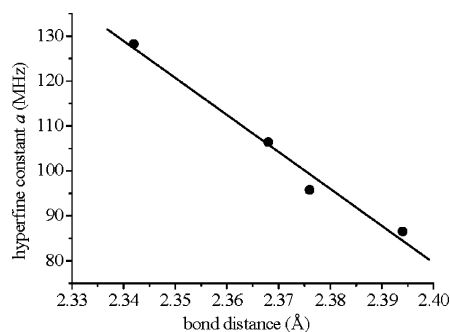


Figure 7. Correlation between the EPR coupling constants a and Ni(I)–P bond lengths in $[Ni(dppf)_2]PF_6$.

A much better simulation of the initial EPR spectrum of **4** (Figure 5, solid line) was obtained on considering the presence of a few percent of the decomposition product $[Ni(dppf)(Me-THF)_x]^+$, as shown in Figure 5 (dashed line B). The combined analysis of the X-ray and EPR data for the d^9 species $[Ni(dppf)_2]^+$ evidences a linear correlation of the metal–phosphorus bond distances with the hyperfine coupling to the ^{31}P nuclei (Figure 7). Such correlation allows us to assign each hyperfine constant a to a specific ^{31}P nucleus, as shown in Table 4.

A similar dependence was previously reported for the d^9 analogues $M(dppf)_2$ ($M = Rh, Ir$)² and suggested for Rh-

(dppe)₂.²⁸ The correlation found in this work allows one to estimate the nickel–phosphorus bond distance in the decomposition product [Ni(dppf)(Me-THF)₂]⁺. Using the average of the *a_P* values for such species at 7 K (176 MHz), the Ni(I)–P bond length would be about 2.28 Å, a value much closer to the average distance found in the 14 crystal structures containing Ni(I)–P bonds (2.253 Å).

Concluding Remarks

The uncommon ability of the organometallic ligand dppf in sustaining the Ir and Rh atoms in the +1, 0, and –1 oxidation states, recently reported by us, has been now confirmed, even though only partially, for Co and Ni. Compound **1** represents a rare example of zerovalent cobalt complex, but unlike its Rh and Ir analogues, Co(dppf)₂ is only moderately stable in solution. This finding contrasts with the stability shown by the series of compounds M(tropp^{ph})₂ (M(0) = Co, Rh, Ir; tropp^{ph} = tropyliene phosphane) recently described.²⁵ The difference between the Co and the congeners appears more evident when the stability of the d¹⁰ species is considered. While the anions [Rh(dppf)₂][–] and [Ir(dppf)₂][–] are indefinitely stable in THF solution, [Co(dppf)₂][–] is rapidly quenched by the solvent to give the hydride HCo(dppf)₂.

Finally, the whole of the chemical and electrochemical observations points convincingly to the thermodynamic instability of [Ni(dppf)₂]²⁺, despite the well-known stability of other square-planar homoleptic Ni(II) diphosphine complexes.²⁶ Since the conversion from an essentially tetrahedral geometry of the NiP₄ moiety found in **4** toward a planar arrangement of the ligands is expected to occur with a decrease of the Ni–P bond distances,²¹ the observed instability of the [Ni(dppf)₂]²⁺ cation can be attributed to the crowding of the bulky dppf ligands which prevents such transformation of the Ni coordination geometry.

Acknowledgment. The Ministero dell'Università e della Ricerca Scientifica e Tecnologica (PRIN 2004: Pharmacological and Diagnostic Properties of Metal Complexes) is gratefully acknowledged. We thank Prof. C. Corvaja for helpful discussions and Dr. A. Brunetta for his valuable help in the synthesis of the Ni(I) complex.

Supporting Information Available: Crystallographic data in CIF form. This material is available free of charge via the Internet at <http://pubs.acs.org>. Crystallographic data for the structure reported in this paper have also been deposited at the Cambridge Crystallographic Data Center as supplementary publication Nos. Copies of the data can be obtained free of charge upon application to CCDC, 12 Union Road, Cambridge, CB2 1EZ U.K. Fax: +44-1223-336-033. E-mail: deposit@ccdc.cam.ac.uk.

IC061185Z

(28) Mueller, K. T.; Kunin, A. J.; Greiner, S.; Henderson, T.; Kreilick, R. W.; Eisenberg, R. *J. Am. Chem. Soc.* **1987**, *109*, 6313.